RSC Advances

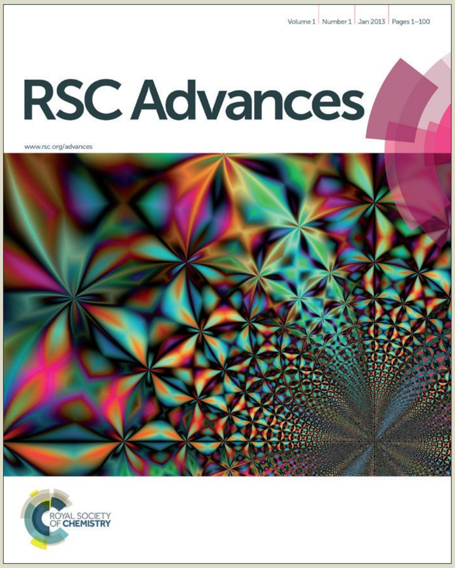

ROYAL SOCIETY OF CHEMISTRY

www.rsc.org/advances

Journal Name

ARTICLE

Energetic Hybrid Polymer Network (EHPN) through Facile Sequential Polyurethane Curation Based on the Reactivity Differences between Glycidyl Azide Polymer and Hydroxyl Terminated Polybutadiene

Abbas Tanver, Fida Rehman, Aisha Wazir [a], Syed Khalid, Song Ma, Xiaoyu Li, Yunjun Luo*, Mu-Hua Huang*

Received 00th January 20xx,
Accepted 00th January 20xx

DOI: 10.1039/x0xx00000x
www.rsc.org/

To improve the thermo-mechanical properties of glycidyl azide polymer (GAP) and hydroxyl terminated polybutadiene (HTPB) based propellants, a facile sequential polymerization approach has been conducted to prepare energetic hybrid polymer network (EHPN) through stepwise curation. The detailed curing conditions for the EHPN formation were carried out by using in-situ FTIR kinetic study. Effect of curing ratio (NCO/OH) on mechanical properties of polyurethane networks of GAP and HTPB has been investigated where, hexamethylene diisocyanate biuret trimers (Desmodur N100) and isophorone diisocyanate (IPDI) as mixed curative agents. A series of EHPNs have been prepared by varying the relative weight ratios of GAP and HTPB with single poly-isocyanate mixed curing system (IPDI/N100). A remarkable mechanical strength up to 5.83 MPa and an elongation at break of 359 % has been achieved with 50:50 weight ratios of GAP to HTPB, which is the maximum mechanical strength reported so far for binder system of GAP and HTPB with thermally more stable cross-linked network. Thermal properties of as-synthesized PU networks of GAP, HTPB and GAP-HTPB EHPNs with different weight ratios were characterized by DMA and DSC techniques. Thermal degradation behavior and morphological studies were also investigated with TGA-DTG and scanning electron microscopy (SEM), respectively. The facile sequential polyurethane curation polymerization technique can be potentially used for advanced solid composite propellants.

Introduction

The state-of-the-art solid rocket propellants are usually contain low-vulnerability binders, which are composed of oxidizers and pre-polymers/ plasticizers, with energetic groups such as $-N_3$ (azido), nitro (C-nitro, O-nitro (nitrate ester) and N-nitro (nitramine)) and difluroamine groups. As a result, the internal energy of the product is enhanced as well as the overall oxygen balance.[1] The polymeric binders in propellants are normally cross-linked polyurethane elastomeric networks functioning as a matrix to bind the solids (such as oxidizers and metal fuels) plasticizers and other minor additives. Among energetic polymers, azido polymers have drawn immense attention for the development of solid propellants. Glycidyl azide polymer (GAP) is an exclusive polymer of high density with positive heat of formation of +117.2 KJ/mol.[2] It outperforms all other azido polymers have been developed during the last decades, due to its positive effect on the specific impulse and burning rate of solid composite propellants through the exothermic $C-N_3$ group scission reaction.[3-6]

GAP is considered as a distinctive contender binder for eco-friendly chlorine-free and smokeless solid propellants.[3,4] However, GAP-based propellants do not reveal good mechanical strength, especially at low temperatures, due to its high chain stiffness from its polyether backbone structure. Normally, the polymeric binder characteristics can significantly influence the structural integrity of the propellant. In order to overcome these problems, many attempts have been made by co-polymerization of GAP with poly ethylene glycol (PEG), poly caprolactone (PCL), tetra hydro furan (THF), ethylene oxide (EO) and HTPB and their mechanical and thermal properties are reported.[7-11] For example, Min et al. Found that the block co-polyurethane binder matrices of GAP/Poly ethylene glycol and GAP/Poly caprolactone were of enhanced mechanical strength.[7] Glass transition temperature of GAP (6 ^{o}C) are much greater than those of HTPB and this considerably limits its application in composite solid propellants. HTPB is widely used as polymeric binder in composite propellant due to its excellent physico-chemical properties.[11-14] HTPB presents low glass transition temperature, hydrolytic stability, high flexibility and resistance to solvents which make it ideal for the composite solid propellant.[15-16] Several research groups have combined HTPB with other pre-polymers to achieve better mechanical, thermal and chemical resistance properties, Interpenetrating polymer networks (IPNs) based on HTPB PU/Poly (methyl methacrylate), HTPB-PU/Polystyrene and HTPB-PU/Poly (ethylene oxide) have been investigated.[17-21]

Many researchers have explored different approaches to improve the mechanical strength of GAP and HTPB, though it is significantly restrained by the poor compatibility between GAP and HTPB due to polar nature of GAP and non polar nature of HTPB.[22] Mathew et al. reported the synthesis of GAP-HTPB cross-linked networks and achieved the mechanical strength around 4.2 MPa and elongation < 200 % with 30 % GAP-MDCI (methylene bis cyclohexyl isocyanate) with two glass transition temperatures at -74.03 ^{o}C and -35.84 ^{o}C.[23] Ding et al. used triazole curing system based on propargyl-terminated polybutadiene (PTPB) and GAP, and reported the maximum mechanical strength up to 2.5 MPa and elongation around 50 % with (N_3 : C≡C) molar ratios of 1 : 2.[2] Bing et al. have achieved 3.83 MPa tensile strength and 593 % elongation by using GAP-HTPB blend binders with 50 : 50 weight ratios but no thermal

---

School of Materials Science and Engineering, Beijing Institute of Technology, Beijing, 100081, China
[a] *Department of Chemistry, Government Samanabad College for Women, Faisalabad, Pakistan*
Correspondence to: yjluo@bit.edu.cn; mhhuang@bit.edu.cn

properties of the as-synthesized GAP-HTPB binder system have been reported.[24] Mohan et al. have synthesized the copolymer of GAP and HTPB, which showed two glass transition temperatures due to incompatibility of polymeric chains. Moreover, only thermal properties of the copolymer was investigated.[8]

In recent years, HPNs have attracted extensive attention which may mingle the properties of components by forming networks and hybrid polymerization signifies an innovative approach to elucidate the problem of polymer incompatibility.[25-31] Normally two kinds of routes are being used, to form HPNs namely sequential and simultaneous polymerization. Sequential polymerization is generally prepared in which second polymeric component network is polymerized following the completion of polymerization of the first component network while Simultaneous polymerization is prepared in which both component networks are polymerized concurrently.[28-32] HPNs have been more and more research attention. This is because of their outstanding properties and synergetic effect introduced by the forced compatibility of the individual components, and thus the enhanced mechanical strength and resistance to thermal degradation resulting from the catenation and entanglements of polymer chains.[33-38]

We have recently reported the preparation of energetic IPNs of azido-alkyne click and polyurethane by using Acyl-GAP and HTPB with dual curing system (DDPM-IPDI/N100) via “simultaneous” polymerization technique to achieve optimum mechanical strength and thermally stable binder system for composite propellants.[39] In order to further simplify the procedure while keep the good mechanical properties, we conducted the facile “sequential” EHPN networks of GAP and HTPB by stepwise curing with single poly-isocyanate mixed curing system (IPDI/N100) as shown in Figure **1**. Comprehensive information regarding curing conditions of GAP and HTPB at the different temperatures was provided by in-situ FTIR kinetic study. Single and inward shifting of glass transition temperatures (*Tg*) was shown by dynamic mechanical analysis (DMA) and differential scanning calorimetry (DSC) and the results from thermo-gravimetric analysis (TGA-DTG) show that the network formed is thermally more stable. IPN with a weight ratio of 50:50 (GAP:HTPB) gave the synergetic mechanical strength, and microscopic studies demonstrates the interlocking and entanglements of GAP-HTPB networks. To the best of our knowledge, our technique for sequential EHPN synthesis is more facile and gave the maximum mechanical strength reported so far for binder system of GAP and HTPB with thermally more stable cross-linked network.

Experimental Section

Materials

GAP with molecular weight 3700 g mol^{-1} and hydroxyl contents 29.15 mg KOH g^{-1}, Nitrogen contents 41.3 %, water contents 0.217 % and functionality 1.92 were purchased from Liming Research Institute of Chemical Industry, Henan, China. HTPB with molecular weight 3020 g mol^{-1}, hydroxyl contents 0.73 mmol g^{-1}, Hydrogen peroxide (H_2O_2) contents 0.022 %, water contents 0.015 % and functionality 2.205 was also purchased from the same supplier and both GAP and HTPB were used after vacuum dried for 3 hours at 80 °C. The average molecular weight of isophorone diisocyanate (IPDI) is 222.2 g mol^{-1} and it contains 9.0009 mmol of NCO per gram IPDI, Hexamethylene diisocyanate biuret trimers (Desmodur N100) molecular weight 725 g mol^{-1} and 5.379 mmol of NCO per gram) and Dibutyl tindilurate (DBTDL) 0.5 % solution in diisooctyl sebacate (DOS) were purchased from Beijing chemical plant.

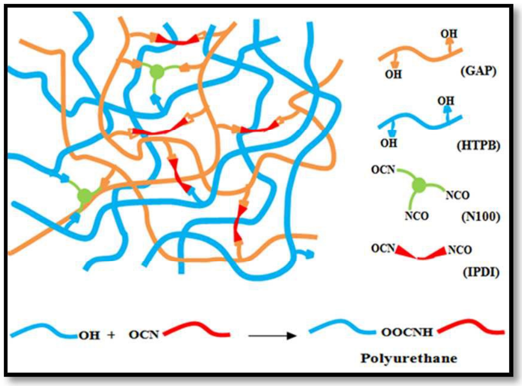

Figure 1: Schematic representation of polyurethane reaction and EIPN structure of PU based on GAP-HTPB.

Preparation of Single Networks

All the reagents were dried overnight in a vacuum oven at 60 °C before use. Polyurethane HTPB network was synthesized by mixing the stoichiometric amount of HTPB, IPDI and N100 in a beaker followed by degassing in a vacuum oven at 30 °C. The equivalent ratio of NCO/OH and IPDI/N100 weight ratio was 1.0. The required amount of DBTDL (0.3 %) was added as a curing catalyst. The mixture was poured into Teflon coated mold and degassed in a vacuum oven. The molds were finally cured at 70 °C for 5 days. Polyurethane GAP network was also prepared by same procedure, except that HTPB was replaced by GAP.

Synthesis of Energetic Hybrid Polymer Network (EHPNs)

GAP-HTPB EHPNs were synthesized by “sequential” polymerization method where pre-polymers, curing agent, cross-linking agent and catalyst were mixed together (same proportions for each network as used in a single network preparation). A series of GAP-HTPB EIPNs were synthesized by varying the relative weight proportions of HTPB (90, 70, 50, 30, and 10 %) with respect to GAP. The required amount of GAP, HTPB along with IPDI, N100 and DBTDL were placed in a beaker followed by degassing in a vacuum oven at 30 °C. The equivalent ratio of NCO/OH and IPDI/N100 weight ratio were also the same as in the single networks. The whole mixture was poured into a Teflon coated mold and degassed in a vacuum oven at 30 °C. The mold was cured at 30 °C for 3 days followed by 70 °C for 5 days for stepwise curing. Schematic illustration for the reaction of GAP and HTPB with single poly-isocyanate mixed curative system (IPDI/N100) has been shown in scheme **1.**

Measurement of Mechanical and Thermal Characteristics

IR spectra were recorded with Nicolet FTIR-8700; Thermo spectrophotometer in the range of 4000-500 cm^{-1}. The mechanical properties including tensile strength (σ_b) and elongation at break (ε_b) of all the dumbbell-shape specimens were determined using universal testing machine (Instron-6022, Shimadzu Co., Ltd.) at a constant rate of 100 mm/min and the results were averaged from five samples. Glass transition temperatureS (*Tg*) were obtained using differential scanning calorimetry (DSC Mettler Toledo DSC1) with heating rate of 10 °C/min over a temperature range of -100 to 50 °C under nitrogen flow of 40 mL/min.

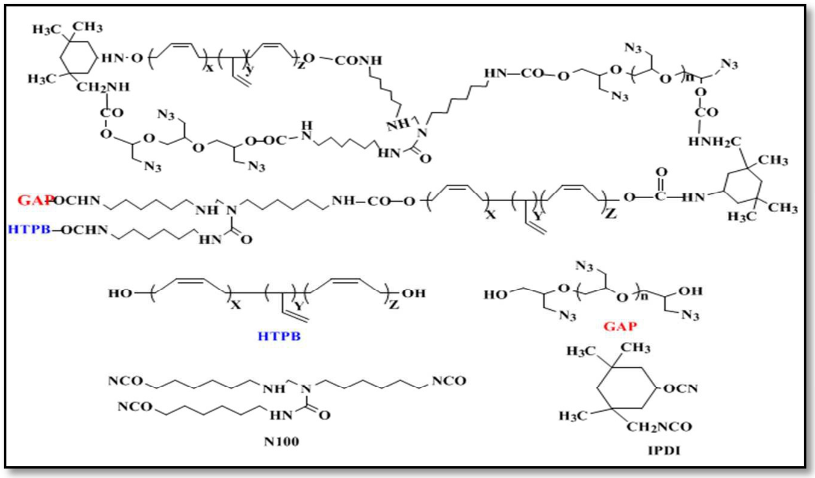

Scheme 1: Schematic illustration for the reaction of GAP and HTPB with mixed curing system IPDI and N100.

Dynamic mechanical tests were performed on a DMA 242C (Netzsch, Hanau, Germany) with a dual cantilever device at a frequency of 1 Hz. The temperature range was from -100 to 50 °C under nitrogen atmosphere with a heating rate of 3 °C/min. The dimensions of the test specimens were 30 mm × 10 mm. Thermogravimetric analysis was performed on TGA analyzer (TGA/DSC1SF/417-2, Mettler Toledo) at a scanning rate of 10 °C/min under nitrogen atmosphere of (40 mL/min) from room temperature (25 °C) to 600 °C. Scanning electron microscopy (SEM) S-4800 (Hitachi) was used in order to image the surfaces of films. All the film samples were fractured with liquid nitrogen and the samples were coated with thin layer of gold before imaging.

Results and Discussion

In-situ FTIR Kinetic Studies of GAP/IPDI-N100 and HTPB/IPDI-N100

In our previous study, it was confirmed that mechanical strength and thermal properties of the GAP could be improved by the incorporation of HTPB via an in-situ polymerization using dual curing system to achieve the energetic Acyl-GAP/HTPB EIPNs.[39] In this work, we investigated the sequential polymerization of GAP and HTPB by controlling the curing conditions. Our group reported In-situ FTIR kinetic studies of GAP/IPDI-N100 and HTPB/IPDI-N100.[40,41] This provided us the kinetic information for the curing reaction, which enables us to adjust the curing conditions for sequential polymerization of EHPN formation.

Figure **2** depicts the reaction kinetics of polyurethane formation in terms of distinctive peaks conversion with respect to time. PU kinetics was followed by observing the change in intensity of absorption band of NCO stretching at 2258 cm^{-1} and CO stretching at 1730 cm^{-1}. Difference in the intensity of peaks was obtained with Omnic software. The intensity of the peak for NCO stretching band decreased and finally disappeared upon completion of the reaction. New absorption peaks at 1731cm^{-1} and 1508 cm^{-1} were assigned to CO and NH stretching band revealed the formation of PU.

In situ FTIR kinetic study shows that around 80 % of HTPB PU network formation completes within 10 hours, where as GAP PU network formation needs almost 80 hours. All the hydroxyl groups of HTPB are primary, while GAP contains around 10 % primary and 90 % of secondary hydroxyl groups. The reactivity of primary hydroxyl groups is higher than that of secondary hydroxyl groups. Moreover the reactivity of NCO groups from N100 (aliphatic) and IPDI (cyclic) are also different. Primary NCO groups of IPDI are almost ten times more reactive then secondary one. There are three primary NCO groups in Desmodur N100 which are more reactive with hydroxyl groups of HTPB and GAP. Figure **3** demonstrates the in-situ FTIR Kinetic study of GAP, HTPB and GAP-HTPB (50:50) at 30 °C. In case of HTPB, almost 95 % polyurethane formation takes place in three days while only 6 % NCO conversion takes place for GAP. In case of GAP-HTPB (50:50) mixed binder systems at 30 °C, almost 52 % NCO conversion takes place and this may be due to reactivity differences of hydroxyl groups of GAP and HTPB. That's why in mixed binder systems (50:50), almost 52 % polyurethane (PU) formation takes place at 30 °C and the remaining NCO conversation takes place at higher temeprature (70 °C). Based on the reactivity differences of hydroxyl and NCO groups of pre-polymers and curing agents, In-situ FTIR Kinetic study motivated us to use sequential polymerization for GAP-HTPB EHPN formation. Although, it does not follows 100 % sequential, on the basis of step wise curation, we can say that sequential polymerization takes place in glycidyl azide polymer and hydroxyl terminated polybutadiene. During first three days curing at 30 °C, most of the HTPB PU network formed while modest amount of GAP PU network formed. The second step curing at 70 °C for five days ensures the

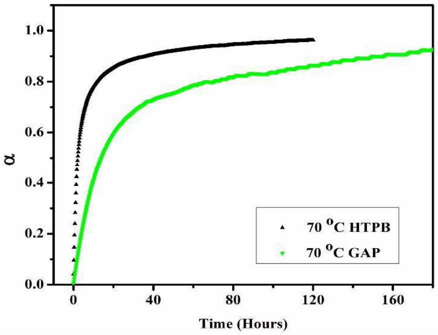

Figure 2: NCO conversion degree-time curves for GAP and HTPB with IPDI/N100 at 70 °C.

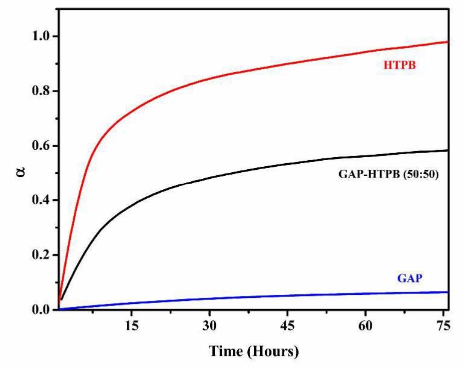

Figure 3: NCO conversion degree-time curves for GAP, HTPB and GAP-HTPB with IPDI/N100 at 30 ^{o}C.

complete PU network formation of GAP and HTPB. This stepwise curing enables the entanglements and cross-linking of both PU networks and effect of this catenation has been studied in detail in mechanical and thermal part of this manuscript.

Mechanical Properties

In order to study the influence of polymerization and cross-linking on GAP/IPDI-N100 and HTPB/IPDI-N100 curing and how these influence the mechanical properties of binder system, we need to investigate the curing system by performing a series of uniaxial tensile tests without solid loading and non-plasticized polymer samples. Shown in figure **4** and **5** are stress strain data of the GAP/IPDI-N100 and HTPB/IPDI-N100 at varying curing ratios (NCO/OH). These tests sequences functioned as a sort of reference for additional evaluations as predicted. Mechanical strength was increased and the elongation correspondingly decreased with increasing curing ratios. Figure **4** shows that by increasing the curing ratio (NCO/OH) from 0.8 to 1.8 in GAP/IPDI-N100, tensile strength gradually increased from 0.35 to 0.93 MPa while the breaking elongation decreased from 280 to 104 %. (NCO/OH) ratio > 1 in both GAP and HTPB binder system, tensile strength gradually increased on the expense of elongation due to higher cross-linked density, which restricts the chain mobility.[42] As a result of that, breaking elongation decreased and tensile strength increased by increasing the curing ratio (NCO/OH). The same trend was observed in HTPB/IPDI-N100 curing system (Figure **5**) in which the tensile strength progressively increased from 1.33 to 2.11 MPa and elongation dropped from 590 to 267 %. Figure **6** depicts the dependence of tensile strength (σ_b) and elongation at break (ε_b) of GAP-HTPB EHPNs. Pure GAP and HTPB urethane network shows the tensile strength (σ_b) of 0.56 and 1.48 MPa, and breaking elongation (ε_b) of 194 and 463 % respectively.

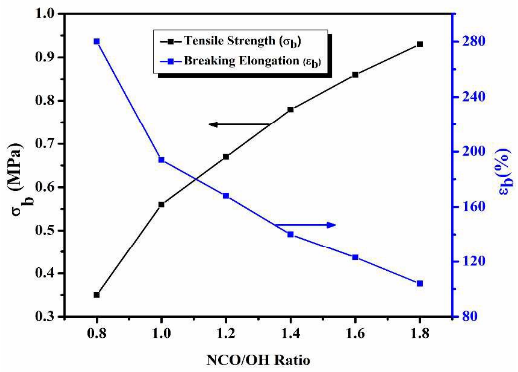

Figure 4: Effect of curing ratio (NCO/OH) on the tensile strength (σ) and breaking elongation (ε_b) of GAP.

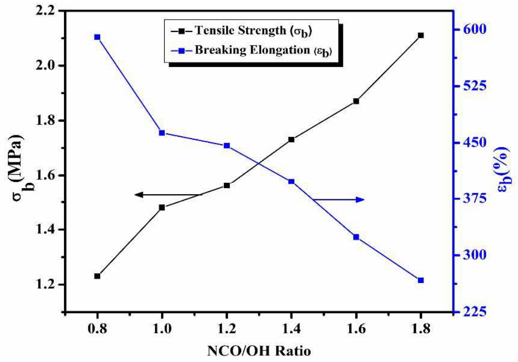

Figure 5: Effect of curing ratio (NCO/OH) on the tensile strength (σ) and breaking elongation (ε_b) of HTPB.

Here we also chose a curing ratio (NCO/OH) of 1.0. As we have mentioned above, sequential polymerization was adopted for HPN formation. Figure **6** shows that by increasing the weight ratio of GAP, tensile strength firstly increased from 1.48 MPa to 5.83 MPa and then steadily decreased to 0.56 MPa, but breaking elongation gradually decreased from 463 to 194 %. An extensive increase in tensile strength and decrease in breaking elongation occurred during sequential polymerization. Figure **1** & **2** (Supporting information) clearly demonstrate the effect of curing ratio (NCO/OH) on the crosslinking density and swelling behavior of the GAP and HTPB respectively. Figures **1** and **2** show almost the same trend of crosslinking density where crosslinking density increased with the increase in NCO/OH ratio while swelling ratio decreased. The increase of crosslinking points can inhibit the swelling behaviour. NCO/OH ratio > 1 in both GAP and HTPB binder system, tensile strength gradually increases on the expense of elongation due to formation of more stiff structure; more PU linkage takes place between hydroxyl groups of GAP and HTPB, which restricts the chain mobility. As a result of that, matrix takes more loads with less breaking elongation. In general, higher crosslinking density results in higher tensile strength and lower elongation at break, that's why with the increase in NCO/OH ratio, crosslinking density increased with an increase in tensile strength while the breaking elongation decreased with the decrease in swelling ratio.

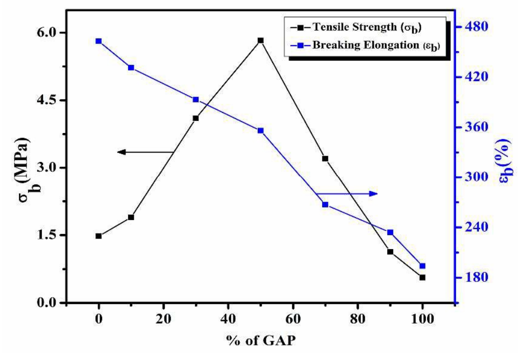

Figure 6: Effect of % of GAP on the tensile strength (σ) and breaking elongation (εb) of GAP-HTPB EHPNs

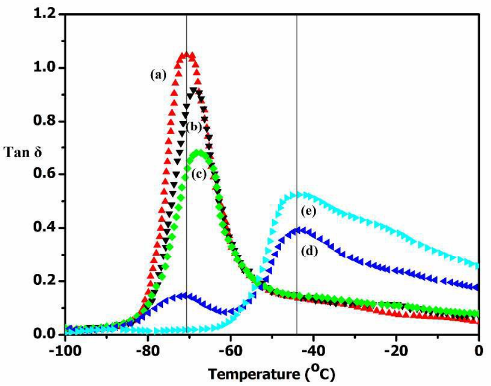

Figure 7: Variation of tan δ with temperatures on (a) 0 %, (b) 10 %, (c) 30 % (d) 50 %, (e) 70 % GAP in GAP- HTPB EHPNs.

Tensile strength 5.83 MPa with 359 % elongation was achieved with 50:50 % of GAP-HTPB EHPNs. Similar trend of crosslinking density has been observed; where as the figure **3** (supporting information) also represents the maximum crosslinking with 50:50 % GAP-HTPB EHPNs. This enhanced mechanical strength may be attributed to the hybrid network formation of GAP and HTPB. Due to catenation, chain flexibility is extremely restricted and elongation at break is considerably reduced. Beyond 50 % GAP, the elasticity of GAP is inhibited by the azido groups and tensile strength and elongation at break gradually drops down to 0.56 MPa and 194 % respectively with 100 % GAP network.

Thermal Studies

Dynamic Mechanical Analysis

Dynamic mechanical properties of GAP-HTPB EHPNs with GAP contents 0, 10, 30, 50 and 70 % were characterized. Samples with 90 and 100 % GAP contents could not be analyzed at specific frequency because samples were broken down from terminal in the sample holder due to low mechanical strength. Curing ratio (NCO/OH) for all samples has been used as 1. Figure **7** depicts the variation in Tan δ and glass transition temperatures (*Tg*) with weight ratio of GAP and HTPB.

Figure **7** also shows that inward shift of glass transition temperature took place from – 71 ^{o}C to – 68 ^{o}C with a single glass transition temperature, where as with 50:50 weight % of GAP-HTPB HPNs, two glass transitions were observed at – 71 ^{o}C and -44 ^{o}C. The results from DMA tests clearly shows that HPNs with GAP up to 30 % did not show phase separation with a single broad transition and maximum Tan δ (1.05). Beyond 30 %, the two glass transition temperatures might be due to phase separation. But surprisingly synergetic mechanical strength was observed at 50:50 GAP-HTPB. Again with 70 % GAP, single glass transition observed and this inward shifting of *Tg* and Synergetic mechanical strength were observed. All these may be attributed to the interpenetration and entanglements of GAP and HTPB networks during sequential polymerization.

TGA/DTG Analysis

TGA/DTG studies for composite propellants can reveal their crucial performance parameters, such as heat of explosion, detonation energy and detonation velocity.[43,44] Figure **8** depicts the TGA thermo gram of GAP, HTPB and GAP-HTPB cross-linked networks. TGA thermo gram of GAP illustrates weight loss in two stages. The first stage decomposition of GAP took place in the temperature range of 191–270 ^{o}C with a weight loss of 39 % due to release of nitrogen,[3,8] while the second stage decomposition involves the degradation of polyether main chain of GAP in the temperature range of 271–468 ^{o}C. The residue remains around 30 % after the complete decomposition of pure GAP network.[23] Cross-linked HTPB network decomposition also occurs in two stages with indefinite division. The first stage decomposition took place with a mass loss of 22 % in the range of 212 to 417 ^{o}C as a result of depolymerization, cyclization and incomplete decomposition of cyclized products. Second stage decomposition occurred in the range of 417 to 492 ^{o}C correspond to dehydrogenation and decomposition of the remaining cyclized products.[45-47]

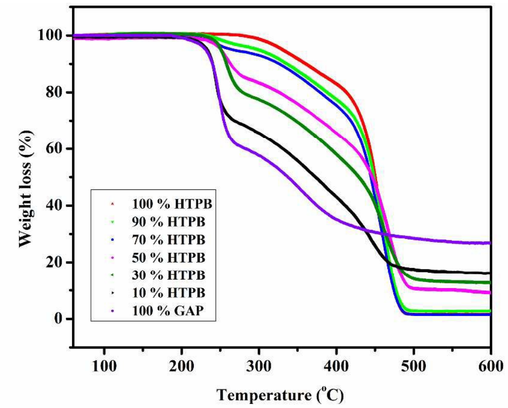

Fig 8: TGA curves of GAP, HTPB and GAP-HTPB EHPNs

Residue after complete decomposition is around 1 %. With increasing weight ratio of GAP, thermally more stable network was formed and decomposition temperatures increased as clearly depicted in the DTG thermo grams (Figure **9**). With 50 and 70 % GAP weight ratios in GAP-HTPB EHPNs, the second stage decomposition increased to 501 ^{o}C and peak decomposition temperatures also increased as depicted in Figure **9**. Variation in decomposition may be ascribed to higher cross-linked networks and the resultant catenation. It can be seen from DTG curves that during the first, peak decomposition temperatures changed from 250 ^{o}C to 259 ^{o}C and from 458 ^{o}C to 468 ^{o}C during the second stage. Higher the cross-linked network, more energy is needed for decomposition.[2]

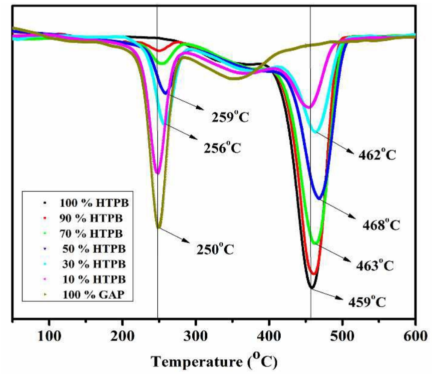

Fig 9: DTG curves of GAP, HTPB and GAP-HTPB EHPNs

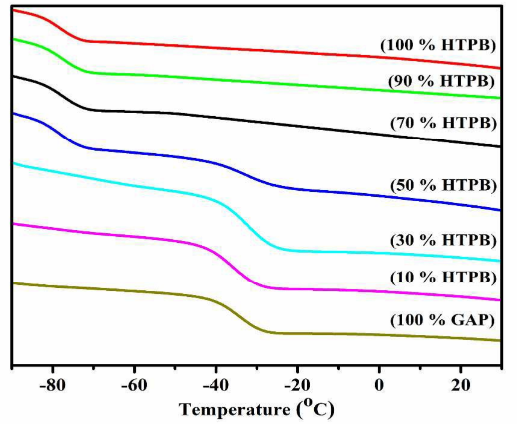

Figure 10: DSC thermo grams of HTPB, GAP and GAP-HTPB EHPNs

DSC Analysis

Figure **10** shows the DSC thermo grams of the pure GAP, HTPB and GAP-HTPB EHPNs with different weight ratios. The glass transition temperature (*Tg*) of the pure HTPB and GAP networks was found to be -76 °C and -36 °C respectively. With the increase in weight ratio of GAP up to 30 %, only one T_g was observed and also slightly increased from -76 °C to -72 °C. This may be attributed to entanglements and interlocking of polymer networks and reduction of gap between cross-linking sites. DSC thermo gram with 50:50 % GAP-HTPB weight ratio shows two glass transition temperatures at -74 °C and -37 °C, which might be due to phase separation but fortunately mechanical properties were enhanced. Same trend of inward shifting of T_g was observed from 70 to 100 % GAP cross-linked network. The characterization for impact, friction and electrostatic discharge sensitivities of the EHPNs and single networks of GAP and HTPB were performed using standard procedure[48] and results clearly showed that single networks of GAP, HTPB and GAP-HTPB EHPNs were insensitive to impact, friction and ESD with > 40 Joules, > 360 Newton and having no ignition at 5.5 Joules respectively.

Morphological studies

Figure **11** shows the morphological characteristics of fractured surfaces of single networks of GAP, HTPB and GAP-HTPB EHPNs. The images of GAP and HTPB are shown in figure **11**-A & B, respectively. It can be seen that fractured surface of single network of GAP shows smooth and glassy microstructures whereas HTPB shows rough, wrinkle and ravine microstructures. SEM images of GAP-HTPB cross-linked networks (11-C & D) depict interlocking and entanglements due to interpenetration of networks; wherein, polymer chains emerge to penetrate inward and outward over one another in polymer matrix and showed interlocking and compact network with good compatibility.[49-51] We also examined micro to nanometre thick long strands which are crossed and entangled with each other. The synergetic mechanical strength, thermally more stable networks, inward shifting of *Tg* and increase of peak decomposition temperatures have been significantly investigated during sequential polymerization of GAP and HTPB with step wise curing by controlling the temperature conditions.

Conclusions

The polyurethane curation of GAP and HTPB with isocyanate was comprehensively investigated by in-situ FTIR, which resulted in the optimization of polymerization conditions. Base on this, a facile sequential polymerization approach for energetic hybrid polymer network (EHPN) formation of GAP and HTPB has been achieved by stepwise curation. Thermo-mechanical properties have been investigated by varying curing ratios (NCO/OH) for single networks of GAP and HTPB. By screening the GAP to HTPB weight ratio (1:9, 3:7, 5:5, 7:3 and 9:1) in the EHPN formation, the superior mechanical characteristics have been achieved with 50:50 GAP-HTPB weight ratios. DMA and DSC studies revealed that inward shifting of glass transition temperatures around 3-4 °C observed with mostly single *Tg* and TGA-DTG studies demonstrated that the network formed were thermally more stable. Peak decomposition temperatures increased by almost 10 °C. Morphological study illustrated that compact networks were formed due to interlocking and catenation of both GAP and HTPB due to sequential polymerization.

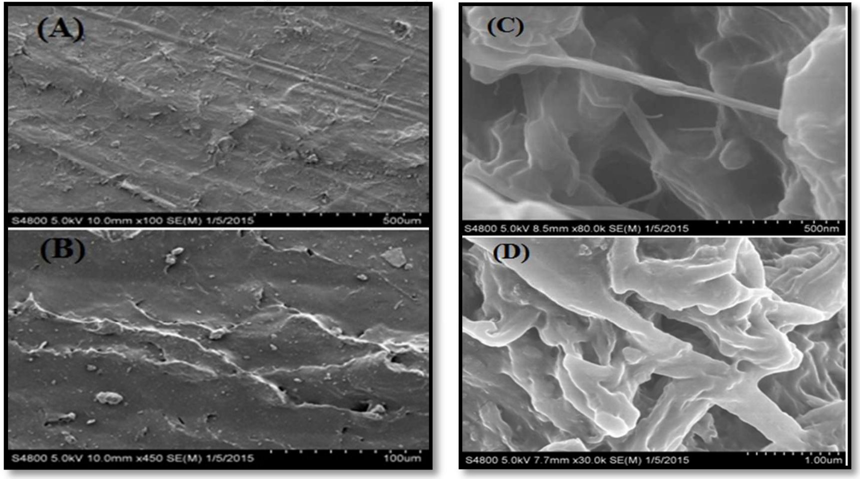

Figure 11: SEM images for the fractured surfaces of the films coded as (A) GAP PU (B) HTPB PU (C-D) 50:50 % GAP-HTPB PU EHPNs

References

1. Provatas, A. *A. Energetic Polymers and Plasticizers for Explosive Formulation—A Review of Recent Advances*; DSTO-TR-0966, Defence Science & Technology Organization, Melbourne, Australia, 2000.
2. Ding, Y.; Hu, C.; Guo, X.; Che, Y.; Huang, J. *J. Appl. Polym. Sci.* 2014, **131**, 40007.
3. Selim, K.; Özkar, S.; Yilmaz, L. *J. Appl. Polym. Sci.* 2000, **77**, 538-546.
4. Kasıkçı, H.; Pekel, F.; Özkar, S. *J. Appl. Polym. Sci.* 2001, **80**, 65-70.
5. Murali Mohan, Y.; Padmanabha Raju, M.; Mohana Raju, K. *J. Appl. Polym. Sci.* 2004, **93**, 2157-2163.
6. Manu, S. K.; Varghese, T. L.; Mathew, S.; Ninan, K. N. *J. Appl. Polym. Sci.* 2009, **114**, 3360-3368.
7. Sun Min, B. *Propellants, Explos., Pyrotech.* 2008, **33**, 131-138.
8. Mohan, Y. M.; Raju, K. M. *Des. Monomers Ploym.* 2005, **8**, 159.
9. Davenas, A. *J. Propul. Power.* 2003, **19**, 1108-1128.
10. DeLuca, L. T.; Galfetti, L.; Maggi, F.; Colombo, G.; Merotto, L.; Boiocchi, M.; Paravan, C.; Reina, A.; Tadini, P.; Fanton, L. *Acta Astronaut.* 2013, **92**, 150-162.
11. Abkay, M. K.; Davendra, P. D. *Res. J. Chem. Environ.* 2010, **14**, 94–103.
12. Badgujar, D. M.; Talawar, M. B.; Asthana, S. N.; Mahulikar, P. P. *J. Hazard. Mater.* 2008, **151**, 289-305.
13. Assink, R. A.; Lang, D. P.; Celina, M. *J. Appl. Polym. Sci.* 2001, **81**, 453-459.
14. Hailu, K.; Guthausen, G.; Becker, W.; König, A.; Bendfeld, A.; Geissler, E. *Polym. Test.* 2010, **29**, 513-519.
15. Sekkar, V.; Bhagawan, S. S.; Prabhakaran, N.; Rama Rao, M.; Ninan, K. N. *Polym.* 2000, **41**, 6773-6786.
16. Xie, H.-Q.; Guo, J.-S. *Eur. Polym. J.* 2002, **38**, 2271-2277.
17. Plesse, C.; Vidal, F.; Gauthier, C.; Pelletier, J.-M.; Chevrot, C.; Teyssié, D. *Polym.* 2007, **48**, 696-703.
18. Wang, S. H.; Zawadzki, S.; Akcelrud, L. *J. Polym. Sci., Part B: Polym. Phy.* 2000, **38**, 2861-2872.
19. Roha, M.; Dong, F. *J. Appl. Polym. Sci.* 1992, **45**, 1397-1409.
20. Jia, D. M.; You, C. J.; Wu, B.; Wang, M. Z. *Int. Polym. Process.* 1988, **3**, 205-210.
21. Han, M. H.; Kim, S. C. *Polym. Adv. Technol.* 1997, **8**, 741-746.
22. Manu, S. K.; Varghese, T. L.; Mathew, S.; Ninan, K. N. *J. Propul. Power.* 2009, **25**, 533-536.
23. Mathew, S.; Manu, S. K.; Varghese, T. L. *Propellants, Explos., Pyrotech.* 2008, **33**, 146-152.
24. Ni Bing.; Qin Guang ming.; Ran Xiu-lun. *Chine. J. Energ. Mater*. 2010, 18, **2**, 167-173
25. Ajithkumar, S.; Patel, N. K.; Kansara, S. S. *Eur. Polym. J.* 2000, **36**, 2387-2393.
26. Chen, S.; Wang, Q.; Wang, T. *Polym. Test.* 2011, **30**, 726-731.
27. Pissis, P.; Georgoussis, G.; Bershtein, V. A.; Neagu, E.; Fainleib, A. M. *J. Non-Cryst. Solids.* 2002, **305**, 150-158.
28. Gitsov, I.; Zhu, C. *J. Am. Chem. Soc.* 2003, **125**, 11228-11234.
29. Jansen, B. J. P.; Rastogi, S.; Meijer, H. E. H.; Lemstra, P. J. *Macromol.* 1999, **32**, 6290-6297.
30. Nakanishi, H.; Satoh, M.; Norisuye, T.; Tran-Cong-Miyata, Q. *Macromol.* 2004, **37**, 8495-8498.
31. Turner, J. S.; Cheng, Y. L. *Macromol.* 2000, **33**, 3714-3718.
32. Gao, D.; Jia, M. *J. Appl. Polym. Sci.* 2013, **128**, 3619-3630.
33. Hu, Y.-Y.; Zhang, J.; Fang, Q.-C.; Jiang, D.-M.; Lin, C.-C.; Zeng, Y.; Jiang, J.-S. *J. Appl. Polym. Sci.* 2015, **132**. 41537.
34. Chaudhary, S.; Parthasarathy, S.; Kumar, D.; Rajagopal, C.; Roy, P. K. *J. Appl. Polym. Sci.* 2014, **131**, 40490.
35. Wang, J.-J.; Wu, M.-B.; Xiang, T.; Wang, R.; Sun, S.-D.; Zhao, C.-S. *J. Appl. Polym. Sci.* 2015, **132**, 41585.
36. Abbasi, F.; Mirzadeh, H.; Katbab, A. A. *J. Appl. Polym. Sci.* 2002, **86**, 3480-3485.
37. Fichet, O.; Vidal, F.; Laskar, J.; Teyssie, D. *Polym.* 2005, **46**, 37-47.
38. Jayasuriya, M. M.; Hourston, D. J. *J. Appl. Polym. Sci.* 2012, **124**, 3558-3564.
39. A. Tanver.; M. Huang, Y. Luo.; S. Khalid.; T. Hussain*, RSC Adv.*, 2015, **5**, 64478-64485
40. Shen Fei-Fei.; A. Tanver.; Y. Luo, *Chine. J. Explos. Propellants*, 2014, 37, **4**, 14-18
41. A. Tanver.; M. Huang.; Y. Luo.; Z.H. Hei, *Advan. Mater. Res,* 2015*,* **1,** 337-341.
42. Hu, C.; Guo, X.; Jing, Y.; Chen, J.; Zhang, C.; Huang, J. *J. Appl. Polym. Sci.* 2014, **131**, 40007.
43. Herder, G.; Weterings, F. P.; de Klerk, W. P. C. *J. Therm. Anal. Calorim.* 2003, **72**, 921-929.
44. Krabbendam-La Haye.; E. L. M.; de Klerk.;W. P. C.; Miszczak, M.; Szymanowski, J. *J. Therm. Anal. Calorim.* 2003, **72**, 931-942.
45. Ninan, K. N.; Krishnan, K.; Rajeev, R.; Viswanathan, G. *Propellants, Explos., Pyrotech.* 1996, **21**, 199-202.
46. Chen, J. K.; Brill, T. B. *Combust. Flame.* 1991, **87**, 217-232.
47. Simon, J.; Bajpai, A. *Eur. Polym. J.* 2003, **39**, 2077-2089.
48. Miró Sabaté, C.; Delalu, H.; Jeanneau, E. *Chemistry – An Asian Journal* 2012, **7**, 1085-1095.
49. B. T. Low, T. S. Chung, H. Chen, Y. C. Jean, and K. P. Pramoda, *Macromolecules*, **42**, 7042 (2009).
50. Jansen, B. J. P.; Rastogi, S.; Meijer, H. E. H.; Lemstra, P. J. *Macromol.* 1999, **32**, 6290-6297.
51. Desai, S.; Thakore, I. M.; Brennan, A.; Devi, S. *J. Appl. Polym. Sci.* 2002, **83**, 1576-1585.

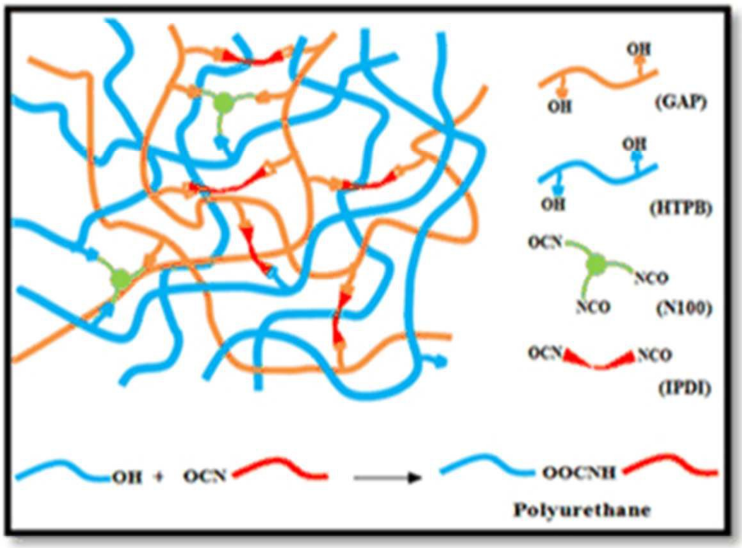

101x101mm (96 x 96 DPI)